

# VARIANT FRICTION COEFFICIENTS OF LAGGING AND IMPLICATIONS FOR CONVEYOR DESIGN

Brett DeVries

Flexible Steel Lacing Company, USA

## SYNOPSIS

For many decades, lagging has been used to both protect conveyor pulleys and to increase the available friction for driving the conveyor belt. Today, lagging is available in various embodiments with differing stated capabilities and strengths.

A primary consideration in the choice of lagging is the coefficient of friction. Designers use the friction coefficient in the Euler Capstan equation to calculate the drive capacity of the conveyor, so the behaviour of lagging friction under real world conditions is of extreme interest. As belt technology innovates with increasing tensions and more power delivered through the drive pulleys, a correct understanding of the source of friction is necessary.

This paper reviews a technique for measuring lagging friction coefficients under typical conveyor belt pressures (35–700 kPa) and discusses the surprising results. It then explores the concept of lagging traction as a more accurate depiction of drive capacity.

## INTRODUCTION

The march of progress is relentless. New conveyor design tools using powerful algorithms can predict the dynamics of increasingly long distance and high tension conveyor belts. Improved power sources like 6 000 kW gearless drives allow more throughput power on a single pulley than ever before. Both are allowing engineers to design larger and more profitable conveyors, which are more demanding of all the components. Pulley lagging is no exception.

Pulley lagging is available in a myriad of styles and materials. The most common types are autoclave rubber, sheet rubber, strip rubber, and ceramic imbedded in rubber (CIR). All exhibit different coefficients of friction by nature of their design, creating a confusing choice for the conveyor designer. Some established design charts for friction exist like those contained in CEMA's *Belt Conveyors for Bulk Materials 7th Ed.*, and the DIN 22101 standard, but they are generalised, come from best practices, and assume a constant coefficient of friction. In contrast, values published by lagging manufactures may vary significantly from the charts. Additionally, there is no standardised test for determining the lagging friction coefficient or an industry standard for applying a safety factor against slippage.

## SETUP

Five different types of cold bond strip lagging were measured to find the coefficient of friction versus increasing pressure. Test conditions were also varied. Each lagging type was measured under conditions termed 'Clean and Dry', 'Wet', or 'Muddy'. A summary of the tests performed can be found in Table 1.

Some of the lagging patterns were a makeup of ceramic tiles and grooved rubber features. The ceramic tiles were 20 mm square with 1 mm diameter by 1 mm tall raised dimples. The rubber compound was a proprietary SBR/BR blend. Pictures of the lagging types are found in Table 2.

		LAGGING TYPES TESTED				
		Full ceramic	Medium ceramic	Diamond rubber ceramic	Diamond rubber	Plain rubber
CONDITIONS						
Clean & Dry		Yes	Yes	Yes	Yes	Yes
Wet		Yes	Yes	Yes	Yes	Yes
Muddy		Yes	Yes	Yes	Yes	No

Table 1. Lagging tests

The full ceramic pattern has ceramic tiles comprising approximately 80% of the available contact area with the belt and the remaining area as channels for the removal of water and solid contaminants. The medium ceramic pattern has ceramic tiles covering 39% of the available contact area and 34% as rubber. The diamond rubber ceramic pattern has ceramic tiles covering 13% of the available contact area and 54% as rubber. The diamond rubber pattern has rubber comprising 67% of the available contact area. The plain rubber pattern has rubber comprising 80% of the available contact area.

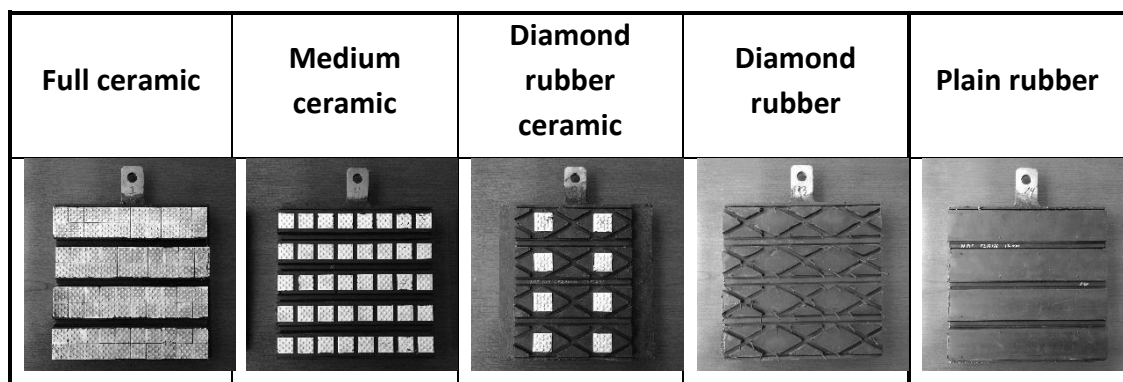


Table 2. Lagging types

## MEASUREMENT

The test fixture was constructed as shown in Figures 1, 2, and 3. It was designed to be used with a standard tensile test apparatus. For these tests an Instron 3369 was used with a 50 kN capacity. The test fixture uses floating pressure plates that are guided by track rails along the bottom edge. Belt samples are secured to the pressure plates such that the bottom covers of the belts face inwardly towards each other. Between the pressure plates is the steel shear plate with lagging samples bonded to it. See Figure 4.

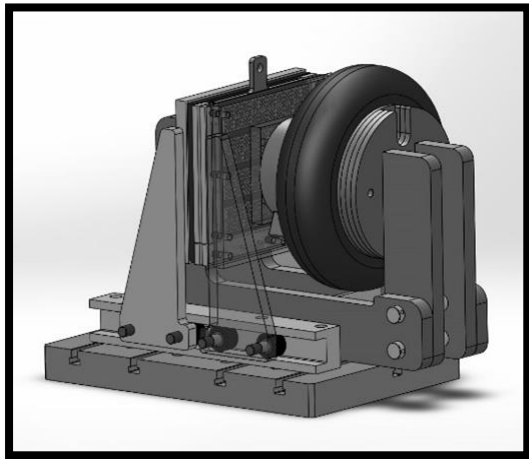


Figure 1. Lagging test fixture

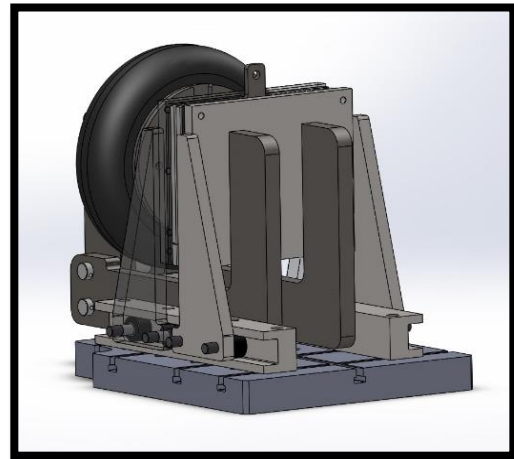


Figure 2. Lagging test fixture

The design of the fixture uses Newton's principle of equal and opposite force reactions to assure the load is equivalent on each side. The pressure plates are substantially thick to prevent flexure. There is a load cell located between the large airbag and the first pressure plate to measure the applied load.

The Instron has a load cell attached to the translating crosshead. This load cell is connected to the sandwiched shear plate via pin connection on the protruding tab.

See Appendix A for a detailed illustration of the entire apparatus. The effective area of the steel shear plate is 412.9 square centimetres. The airbag is capable of applying loads in excess of 28.5 kN, allowing for measurements to 700 kPa if the entire area is used.

The test procedure consisted of placing the shear plate between the pressure plates. Air pressure was then applied and allowed to stabilise to the proper reading. Next, the crosshead translated vertically upward at 50.8 millimetres per minute for a distance of 6.35 mm while data was recorded regarding the position of the crosshead and the vertical load measured by the Instron load cell.

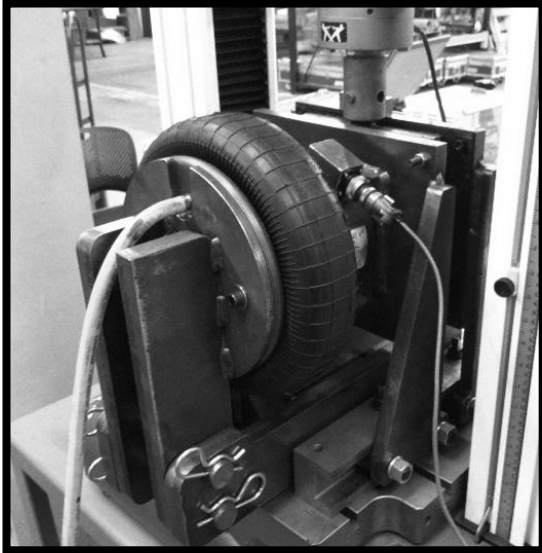


Figure 3. Lagging test fixture in use

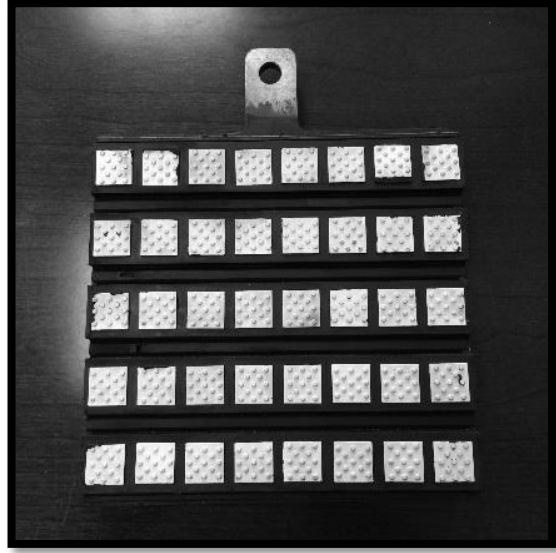


Figure 4. Lagging shear plate with bonded lagging

While the data from the pressure load cell was not dynamically recorded, it was observed from the digital display that it did not vary during the test. Each test was a unique combination of conditions (dry, wet, or muddy), lagging type, and pressure. The test was repeated five times using the same lagging sample for each combination of pressure and conditions and the results averaged. Compressed air was used to blow off debris or dust generated during testing.

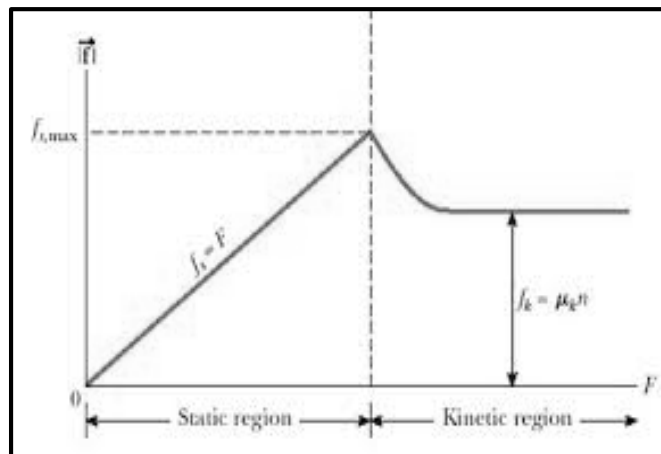


Figure 1. Classic friction behaviour

### RESULTS – STAGE 1

The classic representation of the friction force between two solid objects is that there exists a static coefficient until the start of motion, which then quickly drops to a lesser value known as kinematic friction. Figure 5 illustrates the relationship between applied force and friction.

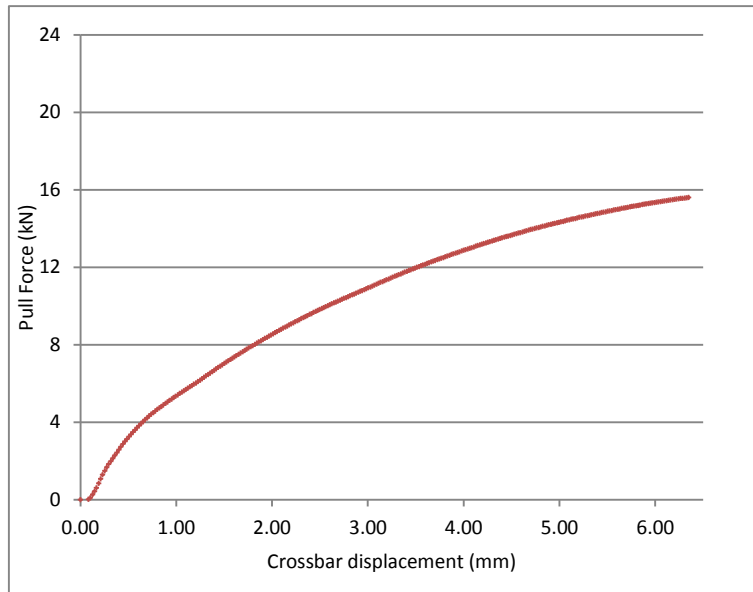


Figure 6. Pull force vs. displacement, 207 kPa, plain rubber lagging, clean and dry conditions

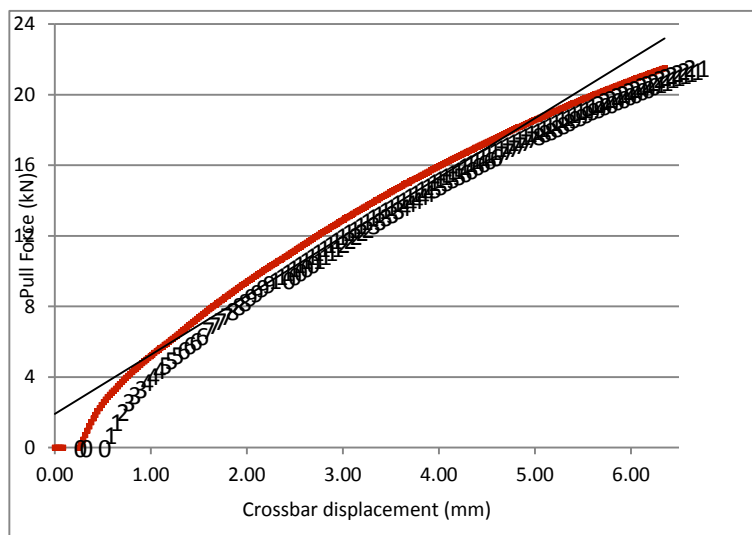


Figure 7. Pull force vs. displacement, 414 kPa, plain rubber lagging, clean and dry conditions

The lagging behaved differently. The first aspect noted upon inspection of the measured extraction force vs. displacement curves was that they did not contain a local maximum force with a rapid decay to a lower value as would occur in classic friction. See Figure 6. Upon visual inspection, it was clear that there had been movement between the lagging and the belt samples, so the absence of a transition was not due to insufficient applied force or displacement. This indicated non-classic friction behavior.

This led to the question of how to measure a friction coefficient at all, since the pull force had not yet stabilised even though slip had clearly been observed.

Another aspect observed was that a doubling in the pressure was not resulting in a doubling of the extraction force. See Figures 6 and 7. This violated classic friction theory which states there is a constant coefficient of friction, which is independent of pressure. The non-linear increase in extraction force also supports the the existence of non-classic coefficient of friction behaviour as observed in the initial test results noted earlier.

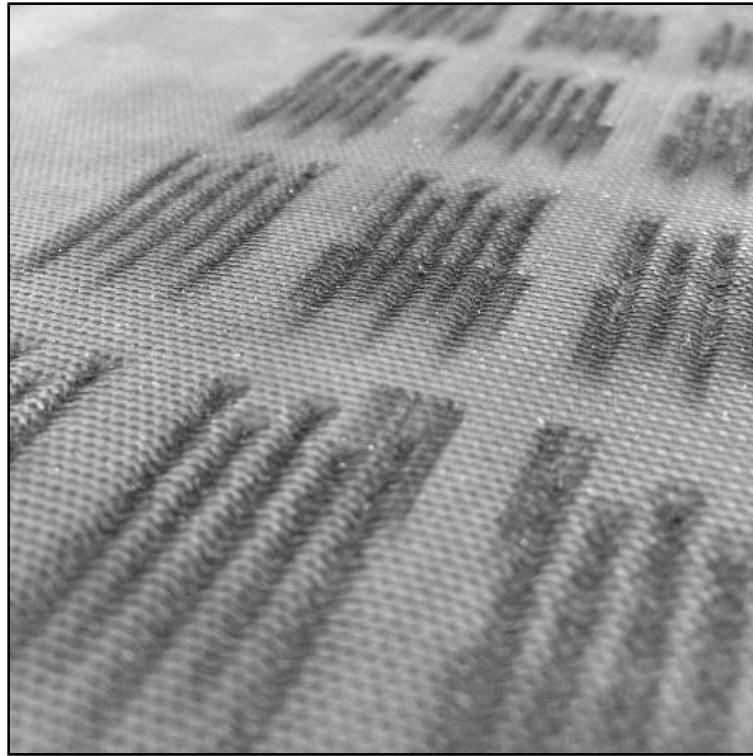


Figure 8. Close up of bottom cover damage

In an attempt to find a static to kinematic friction transition, tests were conducted with the crosshead movement set to 22.23 mm while measuring the extraction force of a ceramic tiled lagging. At this distance, a force maximum was observed with a subsequent fall off, but at a cost of severely damaging the bottom cover of the belt as seen in Figure 8.

After additional research was done regarding the dynamics of a belt traversing a pulley with a 180° wrap, 6.35 mm of crosshead movement was selected as the measurement point for the lagging coefficient. For a more detailed explanation of this selection process, see Appendix B. Later observations of the belt sample pieces used in the tester confirmed that this displacement was reasonable. The same pieces of belt had been used for thousands of tests up to 360 kPa contact pressure, including samples with raised dimple ceramic tiles, and the resulting bottom cover damage was minimal.

## RESULTS – STAGE 2

Using 6.35 mm of crosshead movement as the threshold for developing friction, the coefficient of friction vs. pressure test results of each combination of lagging type and conditions were graphed. Exponential curves were fit to the data to allow for automated calculation of the coefficient of friction. Sample graphs are illustrated in Figures 9 and 10.

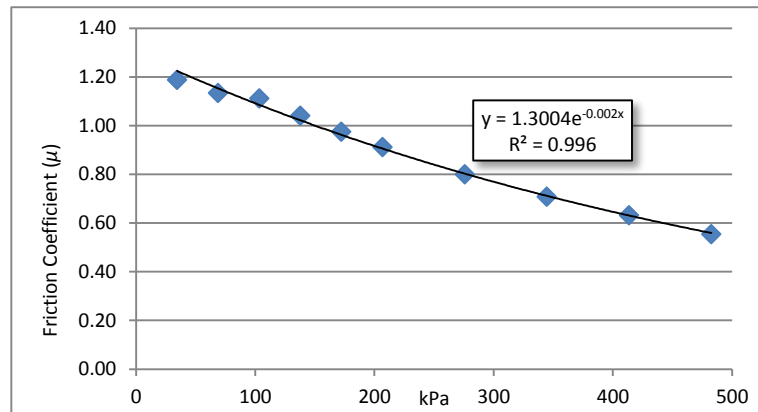


Figure 9. Friction coefficient vs. pressure, plain rubber lagging, clean and dry conditions

The curves showed a general downward trend in coefficient of friction as the pressure increased, except for the medium and full ceramic lagging samples. It was observed that the coefficient of friction peaked at 207 kPa for both. It is inferred that this is the requisite pressure for the 1 mm tall surface nubs to fully engage with the belt. After the peak, the ceramic plots all trended downward like the other samples.

Using the fitted exponential curves, it was possible to consolidate several of the lagging types onto one graph to illustrate the relative friction performance.

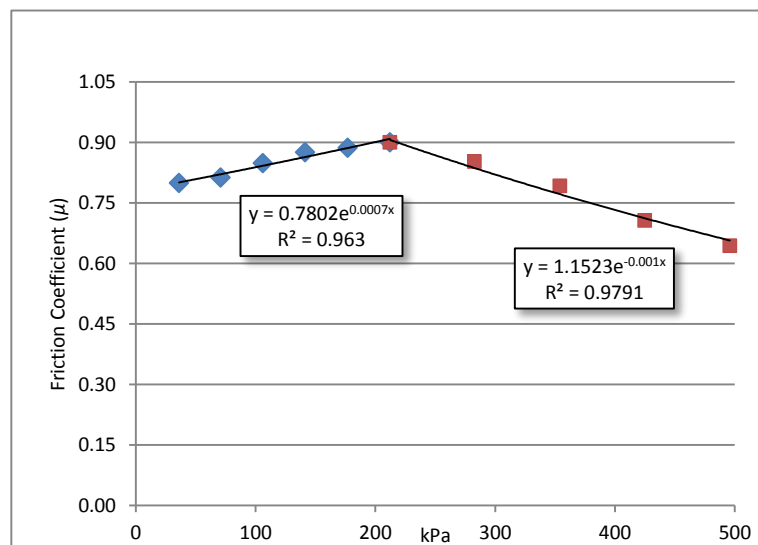


Figure 20. Friction coefficient vs. pressure, full ceramic lagging, clean and dry conditions

Three summary graphs were made. The constant coefficients that existing conveyor belt design standards (CEMA and DIN 22101) assume are also included for reference.

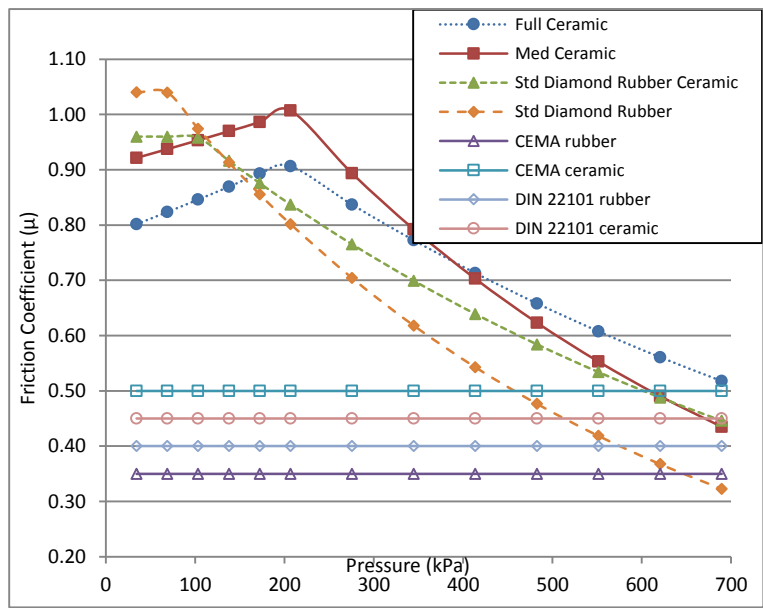


Figure 11. Friction factor vs. pressure, clean and dry conditions

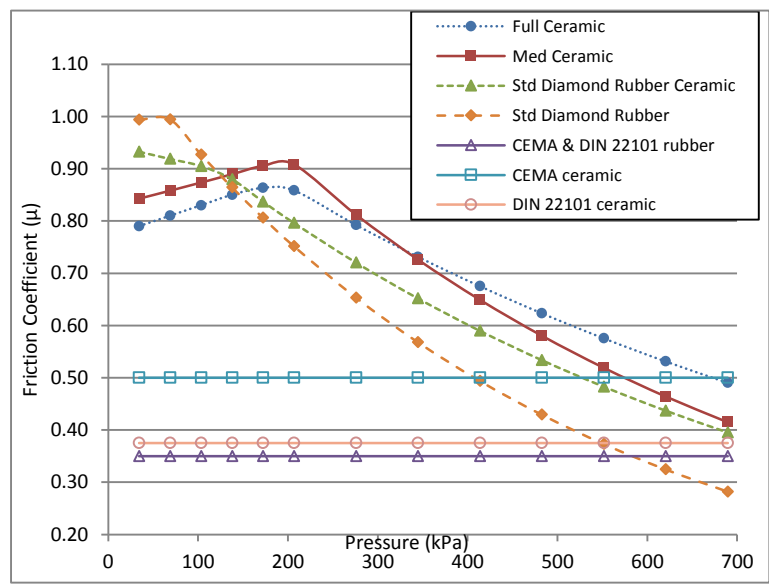


Figure 12. Friction factor vs. pressure, wet conditions

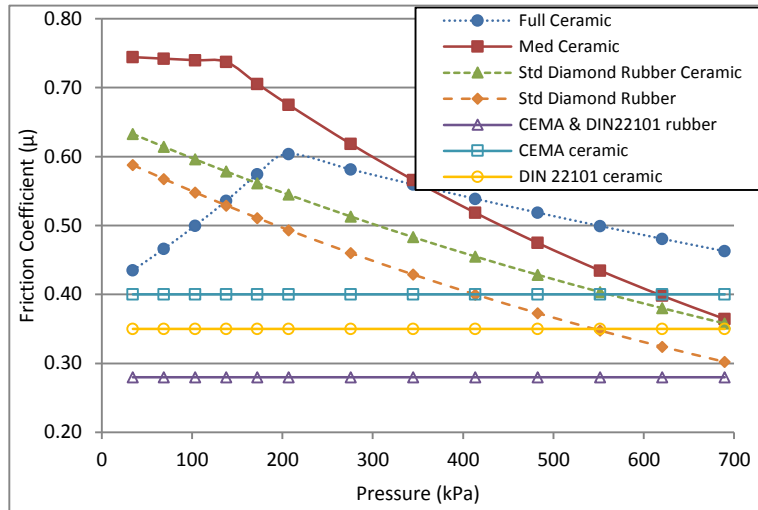


Figure 13. Friction factor vs. pressure, muddy conditions

- Clean and Dry – conditions were as optimal as possible. The lagging and belt were in new condition. See Figure 11.
- Wet – conditions were dew-like. Water was sprayed onto the lagging with a trigger sprayer until water dripped from the lagging. This data does not represent lagging that is hydroplaning or immersed in water. See Figure 12.
- Muddy – samples were painted with an Illinois basin coal fines slurry. The slurry was a mixture of clay and coal particles of unknown distribution. Ratio by weight was 3:2 coal fines to water. See Figure 13.

## DISCUSSION

These results showed a strong dependence of lagging friction on pressure. In practice, pressure arises from the belt tension wrapped around the pulley. From Equation 10, it is seen that wrap pressure is a function of belt tension. Since drive pulleys remove tension from the belt, the results show that the coefficient of friction changes as the belt traverses from  $T_1$  to  $T_2$ . The results also show a 'knee' in most curves with smooth coefficient of friction changes on either side. The smoothness is important since it allows equations to be curve fit. These equations may be used to calculate the expected friction at any discrete point on the pulley.

To explain the significant deviation of the friction coefficient from a classic coefficient of friction paradigm, a modern theory explaining the phenomena of friction is needed. It is worth noting that the classic 'Laws of Dry Friction' were developed between the 15<sup>th</sup> and 18<sup>th</sup> centuries based on scientific observations. They arose from empirical laws rather than from first principles and do not accurately describe the behaviour of some modern materials.

In 1939, F. Philip Bowden and David Tabor showed that at a microscopic level the actual area of contact between two surfaces is much smaller than the apparent area

of contact. Increasing the normal load brings more areas into real contact. (Bowden and Tabor, 1939). B.N.J. Persson showed that rubber friction is the result of both adhesion forces and internal friction. Adhesion causes the rubber to follow the short wavelength surface profile. This deformation of the rubber creates an energy loss governed by the viscoelastic modulus of the rubber and the frequency of the oscillation. (Persson, 1998).

When Bowden and Tabor is applied to rubber, non-classic behaviour is predicted. Since rubber commonly found in belting normally has an elastic modulus of below 6.9 MPa, the area of true contact quickly saturates toward the area of apparent contact at pressures below 700 kPa. Since the area is saturating, the adhesion cannot continue to increase and the ratio of the normal force and sliding force begins to decline. Persson shows that creep movement of the belt against the pulley plays an important role in creating the developed friction.

## APPLICATION

So what should a conveyor designer do? The new data suggests the reason the Euler Capstan equation works is because of generous safety factors in the assumed friction coefficient, especially at pressures below 480 kPa. However, since available friction is pressure dependent, it is difficult to know the actual safety factor and correct results are not assured using this equation when pressures increase.

The Euler Capstan equation expresses the ratio of the incoming and outgoing tensions as an exponential function of the coefficient of friction ( $\mu$ ) and the wrap angle ( $\varphi$ ) in radians

$$\frac{T_1}{T_2} = e^{\mu\varphi} \quad 1$$

The equation is elegant because it does not explicitly calculate the normal force between the belt and pulley. The calculus involved simplifies to just the two tension parameters, but it requires the friction coefficient to be a constant.

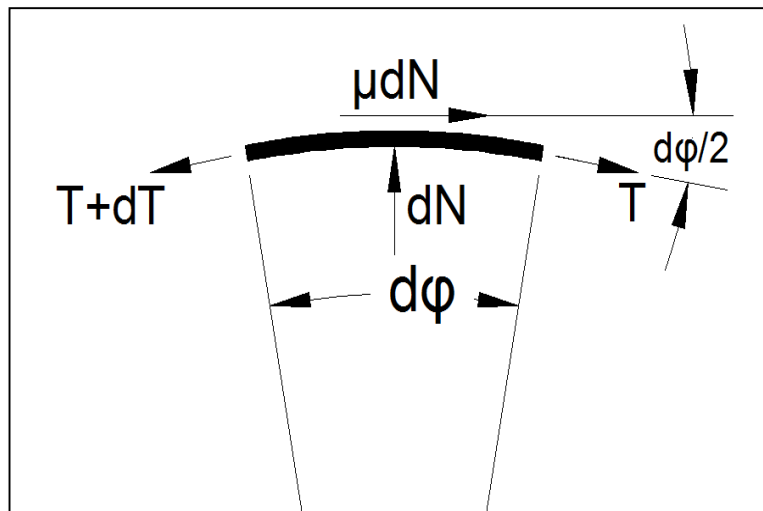


Figure 14. Pulley segment

Consider a small segment of the pulley. Summing the forces in the x-direction

$$T \cos \frac{d\phi}{2} + \mu dN = (T + dT) \cos \frac{d\phi}{2}$$

The x-direction forces simplify to

$$\mu dN = dT \tag{2}$$

Since friction is pressure dependent, friction will have the form

$$\mu = Ae^{bp} dp \tag{3}$$

where  $A$  and  $b$  are constants and  $p$  is wrap pressure.

$dN$  is the normal force against the belt and can be written as pressure multiplied by area, where  $D$  is pulley diameter and  $BW$  is belt width

$$dN = \frac{pD(BW)}{2} d\phi \tag{4}$$

Sum the forces in the y-direction

$$dN = (T + dT) \sin \frac{d\phi}{2} + T \sin \frac{d\phi}{2}$$

Which simplifies to

$$dN = T d\phi \tag{5}$$

Substituting Equation 4 into 5

$$\frac{pD(BW)}{2} d\phi = T d\phi$$

Which simplifies to

$$T = \frac{pD(BW)}{2} \tag{6}$$

Take the derivative of each side

$$dT = \frac{D(BW)}{2} dp \tag{7}$$

By substitution of Equations 3, 4, and 7 into 2

$$Ae^{bp} dp \left( \frac{pD(BW)}{2} d\phi \right) = \frac{D(BW)}{2} dp$$

Which simplifies to

$$d\phi = \frac{1}{A} \frac{e^{-bp}}{p} dp \tag{8}$$

Unfortunately, Equation 8 cannot be solved by conventional means. An approximation method must be employed.

### APPROXIMATION METHOD

Friction force is usually expressed as coefficient of friction multiplied by a normal force. Normal force is distributed over the apparent area of contact and could be expressed as a pressure. So, pressure multiplied by the coefficient of friction is the friction force per unit area between the two apparent areas, otherwise known as shear stress. Conceptually, this could be considered the grip or traction that the lagging has on the belt.

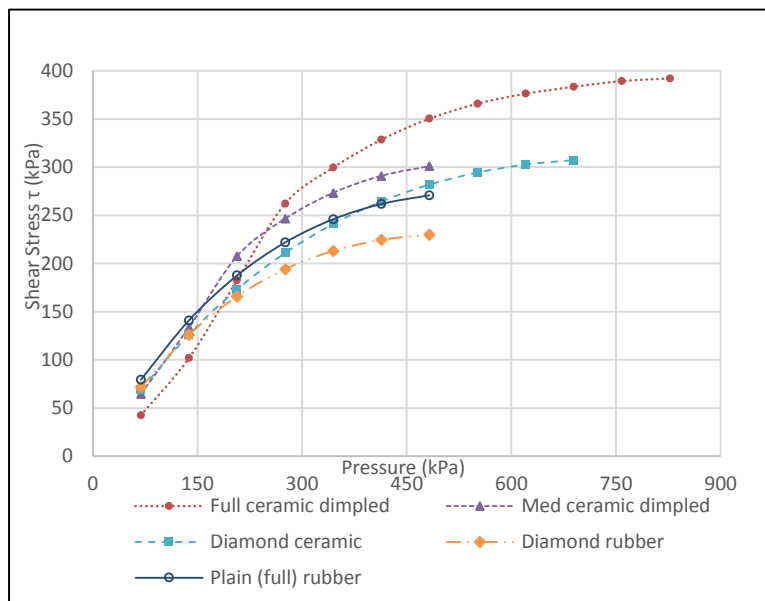


Figure 15. Available driving shear stress, clean and dry conditions

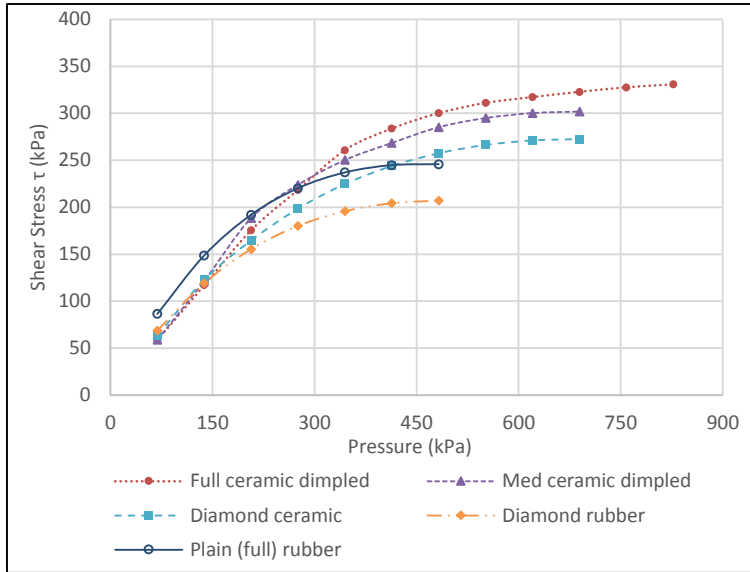


Figure 16. Available shear stress, wet conditions

The shear stress ( $\tau$ ) at the surface junction between the lagging and the belt is  $f(\tau) = pressure * f(\mu)$  9

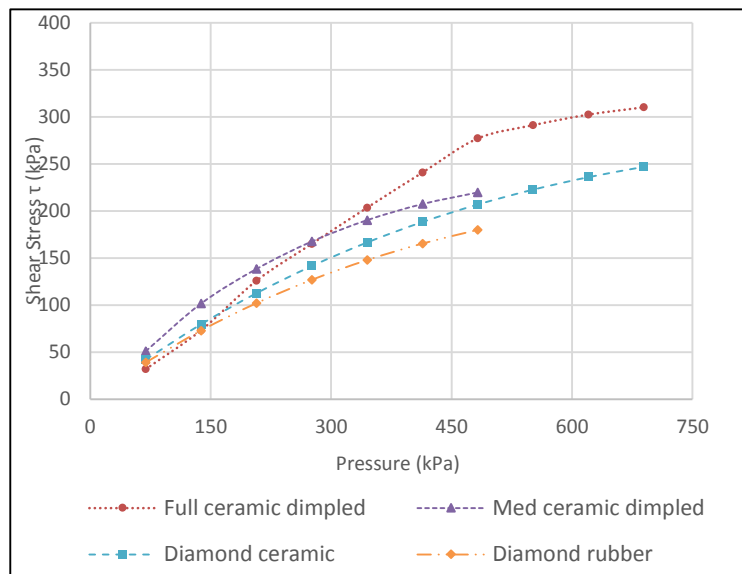


Figure 17. Available shear stress, muddy conditions

Wrap pressure due to tension ( $T$ ) between the belt and the pulley is given by Metlovic (Metlovic, 1996)

$$pressure = \frac{2T}{(BW)D} \quad 10$$

Graphs (Figures 15–17) were made using Equation 9 showing the theoretically available driving shear stress. Curves were created from multiplying pressure by the measured coefficient of friction equations.

As the pressure increases, the available shear stress increases, but at a diminishing rate. The graphs suggest an asymptote for each of the different lagging styles. This is predicted by the origin of the friction force. If the true contact area is approaching the apparent contact area and friction is the result of adhesion forces between the surfaces, then there will be a limit at the maximum shear stress value that those adhesion forces can sustain.

From a practical standpoint, the goal of the conveyor designer is to ensure that the belt can be driven under all foreseeable conditions. One method to achieve this is to use a safety factor. Once the effective shear stress required to drive the belt is known, it can be compared against a theoretical maximum available value and a design safety factor calculated.

The effective shear stress ( $\tau_e$ ) required to drive the belt is related to the effective tension required ( $T_e$ ) by the following equation

$$\tau_e = \frac{2T_e}{\varphi D(BW)} \quad 11$$

where  $\varphi$  is the wrap angle in radians,  $D$  is the diameter of the pulley (with lagging) and  $BW$  is the belt width.

## PROCEDURE

To calculate the safety factor against slip, both the required effective shear stress ( $\tau_e$ ) and the maximum available shear stress ( $\tau_{max}$ ) must be calculated.

- ( $\tau_e$ ) is given by Equation 11.
- Use the graphs to find the available shear stress at  $T_1$  pressure and also at  $T_2$  pressure. Average the result. This average is the theoretical maximum shear stress available to prevent slip defined as  $\tau_{max}$ .

Safety factor is the ratio of the available divided by the required

$$S.F. = \frac{\tau_{max}}{\tau_e} \quad 12$$

It should be noted that there are three ways to increase the safety factor:

- Increase the  $T_1$  tension. As can be seen from the charts, this can be an inefficient way to improve safety factor since the available shear stress increases slowly at higher tensions.
- Change the lagging type. Full ceramic lagging showed the best performance for pressures exceeding 340 kPa.
- Increase the pulley diameter or wrap angle to reduce  $\tau_e$ . From Equation 11 it can be seen that pulley diameter plays a pivotal role in driving the belt as compared to the Euler Capstan Equation 1. With the new method, traction is being increased by placing more lagging area in shear due to the extra circumference generated by a larger diameter.

### DESIGN EXAMPLE

A drive is being designed for belt carrying copper ore in a desert environment. Capacity requirements call for an 1 830 mm belt width with an effective tension,  $T_e$  of 738 kN. Initial specified pulley diameter is 2 200 mm with 15 mm thick lagging.  $T_1$  tension is 1 772 kN and wrap angle is  $186^\circ$ .

- What is the safety factor against slip if dimpled full ceramic lagging is used?
- What is the safety factor against slip if diamond rubber lagging is used instead?
- Using dimpled ceramic lagging and the safety factor from part a), what pulley diameter is required to reduce  $T_1$  to 1475 kN?

**Part (a):** Clean and dry conditions are assumed.

From Equation 11:

$$\tau_e = \frac{2T_e}{\phi D(BW)} = \frac{2 * 738}{186 * \frac{\pi}{180} * 2.230 * 1.830} = 111.4 \text{ kPa}$$

By definition

$$T_1 - T_2 = T_e; \quad T_2 = 1772 - 738 = 1034 \text{ kN}$$

From Equation 10

$$\text{pressure} = \frac{2T}{(BW)D}; \quad p_1 = 868 \text{ kPa}; \quad p_2 = 507 \text{ kPa}$$

Find  $\tau_1$  and  $\tau_2$  on Figure 15 for full ceramic. Since  $p_1$  is beyond the chart, assume the value is equal to the apparent asymptote. In this case,  $\tau_1 = 392$  kPa. From the chart

$$\tau_2 = 358 \text{ kPa.}$$

The average of  $\tau_1$  and  $\tau_2$  is  $\tau_{max} = 375$  kPa. The safety factor is calculated from Equation 12

$$S.F. = \frac{\tau_{max}}{\tau_e} = \frac{375}{111.4} = 3.37$$

**Part (b):** Clean and dry conditions are assumed.

From Equation 11,  $\tau_e$  is the same as Part (a)

$$\tau_e = 111.4 \text{ kPa}$$

From Equation 10, pressures are unchanged

$$p_1 = 868 \text{ kPa}; \quad p_2 = 507 \text{ kPa}$$

Find  $\tau_1$  and  $\tau_2$  on Figure 15 for diamond rubber. Since  $p_1$  and  $p_2$  are beyond the chart, assume the value is equal to the apparent asymptote. In this case

$$\tau_1 = \tau_2 = 230 \text{ kPa.}$$

The average of  $\tau_1$  and  $\tau_2$  is 230 kPa. The safety factor is  $230 \div 111.4 = 2.06$

**Part (c):** Clean and dry conditions are assumed

$T_e$  cannot be adjusted, so the change must come from adjusting  $p_1$ . This is an iterative process and computer assisted solving is recommended. Steps are as follows:

- Guess the pulley diameter should be larger, say 4 inches (approximately 10 cm) bigger.
- Calculate new  $\tau_e$  based on the estimated pulley diameter.
- Desired  $T_1$  is 1475 kN, so  $T_2 = T_1 - T_e = 737 \text{ kN}$ .
- Calculate  $p_1$  and  $p_2$ .
- Using  $p_1$  and  $p_2$ , find  $\tau_1$  &  $\tau_2$  from the charts. Find the average, which is  $T_{max}$ .
- From Equation 12, is the new S.F.  $\geq 3.37$ ? If not, make a new diameter guess and repeat.

To achieve the same safety factor with a  $T_1$  tension of 1 475 kN, the minimum pulley diameter is 2 520 mm.

## CONCLUSION

This improved method for calculating conveyor drive capacity is based on the induced shear stress at the interface of the belt and lagging. It originates from appropriate coefficient of friction data and a modern understanding concerning the origin of rubber friction. It provides the designer with improved accuracy and confidence. Gone are the assumed coefficients of friction that do not match measured data. The improved method also captures and quantifies two intuitive concepts; there is an upper boundary for frictional adhesion and larger pulley diameters have more traction.

A consequence of this approach is the potential for the designer to avoid excessive  $T_1$  tension by increasing the pulley diameter or adjusting the lagging type. Part (c) of the example illustrates this. Since  $T_1$  tension commonly guides the selection of the belt minimum tension rating, reducing it may save on belting costs. Depending on the length of conveyor, large savings may be possible by selecting a lower tension rated (and less expensive) belt and choosing instead to invest in a larger diameter pulley and ceramic lagging.

The new method is easily adaptable to a spreadsheet format where the conveyor designer can choose the best combination of  $T_1$  tension, wrap angle, pulley diameter, and lagging type to optimise their conveyor design.

## APPENDIX A – Instron Test Setup

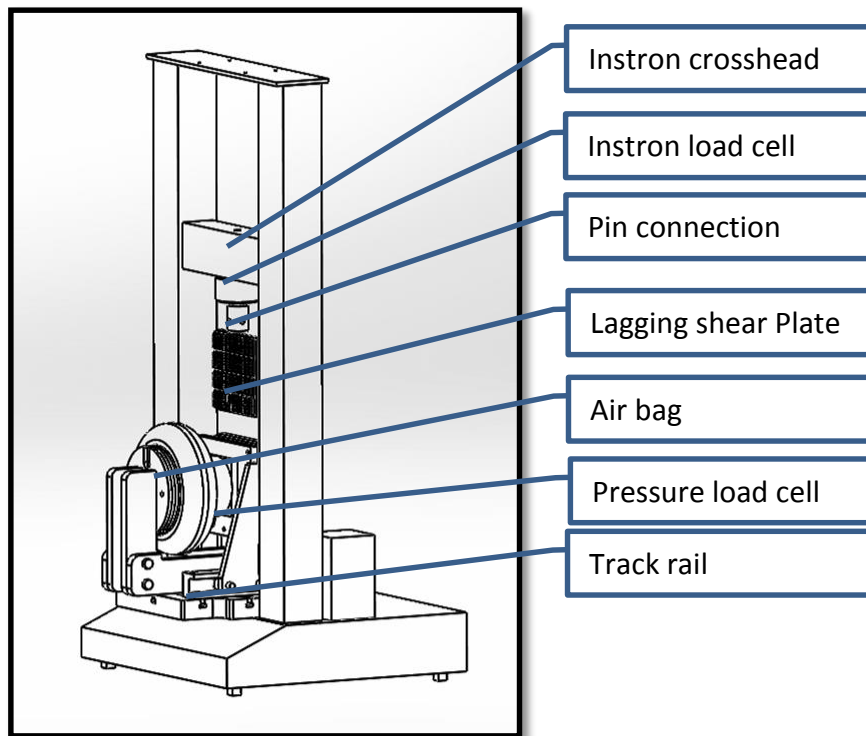


Figure 18. Isometric view

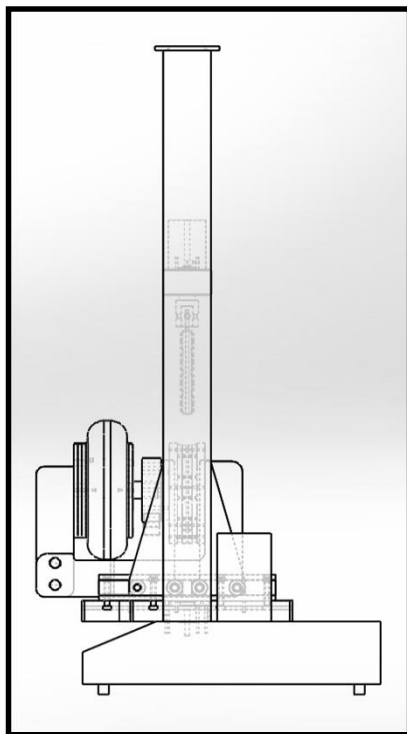


Figure 3. Side view

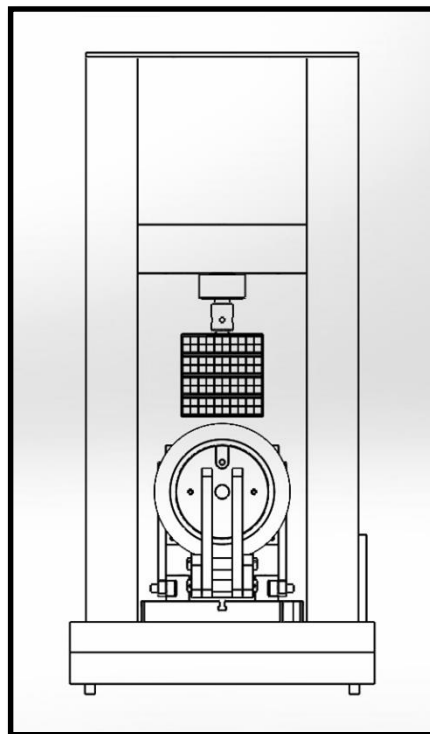
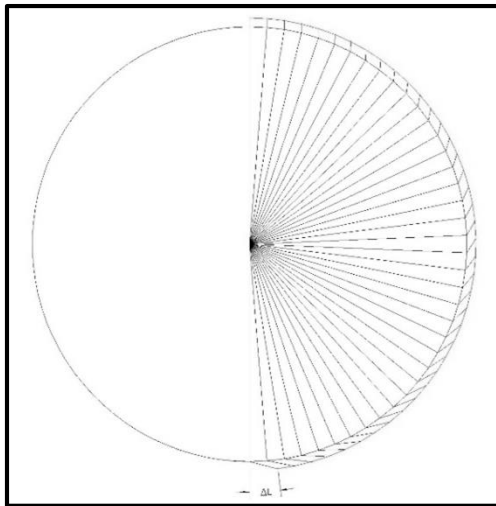


Figure 4. Front view

## APPENDIX B – Pulley Wrap Dynamics

As a belt traverses a drive pulley, the belt carcass has to travel a greater distance than the lagged surface of the pulley. This is due to the extra diameter added by the belt bottom cover and the thickness of the carcass itself.

Consider a belt entering a non-driven pulley. It is well documented that the belt speed and the pulley surface speed are identical. Since no net length change is occurring in the belt, they must have the same exit speed too.



Figure\_21. Accumulated\_length difference

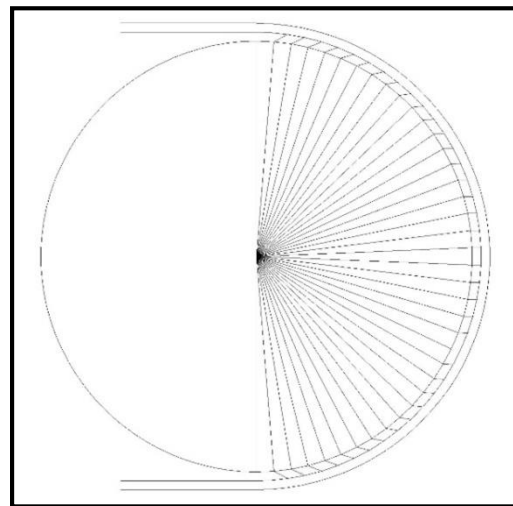


Figure 22. Balanced shear stress

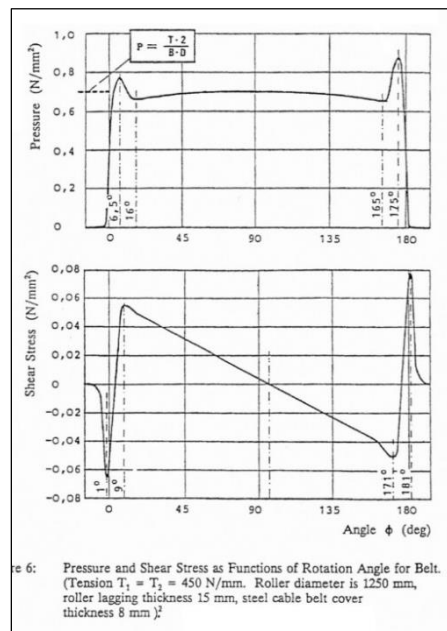


Figure 23. Pressure and shear stress on a non-driven pulley

As the belt wraps around the pulley, the neutral plane of bending is occurring at the midpoint of the thickness of the carcass. This is because the rubber covers are assumed to have negligible influence and the carcass follows standard beam bending theory.

Since the speed is identical, but the belt carcass travel length is greater, the belt cannot traverse the pulley without inducing shear and/or slip.

Imagine that the length differential looks like Figure 21. The outer line represents the mid-plane of the carcass and the angled lines represent increasing shear strain.

However, since the pulley is non-driven, the strain shown in Figure 21 cannot exist since it would take an external torque to sustain in a rubber layer. Instead, the shear stress in the rubber balances itself out by placing the first half of the wrap arc into negative shear. See Figure 22.

Metlovic includes data verifying the balanced stress in the lagging on a non-driven pulley. See Figure 20. Note the slight crest in the pressure graph due to the lagging shear stress changing the belt tension. The spikes at the nip points are due to forces involved with bending the belt.

Driven pulleys have the same differential length issue. Adding torque to drive the pulley will affect the distribution of the shear stresses, but the slip still must be occurring.

The shear displacement due to this effect can be calculated from the following inputs:

$$D = \text{Pulley diameter}$$

$$L_t = \text{Lagging thickness}$$

$$BC_t = \text{Belt cover thickness}$$

$$C_t = \text{Belt carcass thickness}$$

$$\varphi = \text{Wrap angle in radians}$$

Arc length of the lagging surface

$$(D + 2L_t)\pi \times \frac{\varphi}{2\pi}$$

Arc length of the belt carcass

$$(D + 2L_t + 2BC_t + C_t)\pi \times \frac{\varphi}{2\pi}$$

Let total length differential ( $\Delta L$ ) be the difference. Upon inspection

$$\Delta L = (2BC_t + C_t) \times \frac{\varphi}{2}$$

- Does not depend on pulley diameter
- Does not depend on lagging thickness
- Entirely dependent on belt dimensions

- Total length differential results in shear displacements occurring around the pulley with  $\frac{1}{2}\Delta L$  going in the positive shear direction and  $\frac{1}{2}\Delta L$  going in the negative shear direction.

A typical four-ply, 77 N/mm fabric belt has a carcass thickness of 4.30 mm and a minimum bottom cover thickness of 1.5 mm. Using the formula above and an assumed 180° wrap angle, the total length differential would be 11.5 mm with 5.8 mm displacement in both the positive and negative directions. Some of this displacement will result in lagging shear stress and some as slip. Note, this is less than the assumed 6.35 mm displacement used in the friction studies.

A typical four-ply, 175 N/mm fabric belt has a carcass thickness of 8.56 mm and a minimum bottom cover thickness of 1.5 mm. Using the formula above and an assumed 180° wrap angle, the total length differential would be 16.4 mm with 8.2 mm displacement in both the positive and negative directions. Some of this displacement will result in lagging shear stress and some as slip. Note, this has likely more slip than the assumed 6.35 mm displacement used in the friction studies.

A typical ST1600 belt has a cord diameter of 5.6 mm and a minimum bottom cover thickness of 5.0 mm. Using the formula above and an assumed 180° wrap angle, the total length differential would be 24.5 mm with 12.2 mm displacement in both the positive and negative directions. Some of this displacement will result in lagging shear stress and some as slip. Note, this has likely more slip than the assumed 6.35 mm displacement used in the friction studies.

## REFERENCES

- 1 Bowden, F. & Tabor, D., 1939. The area of contact between stationary and between moving surfaces. *Proc. R. Soc. A*, Volume 169, pp. 391-413.
- 2 Metlovic, P. M., 1996. *Mechanics of Rubber Covered Conveyor Rollers*, Akron, OH: Ph.D. Dissertation: The University of Akron.
- 3 Persson, B., 1998. On the theory of rubber friction. *Surface Science*, Volume 401, pp. 445- 454.

## ABOUT THE AUTHOR



### BRETT DEVRIES

Brett DeVries is Chief Engineer of Research and Development of conveyor belt accessories for Flexible Steel Lacing Company (FLEXCO), a US-based multinational company specializing in maximising belt conveyor productivity. Mr. DeVries holds an ABET accredited Bachelor of Science in Mechanical Engineering degree from Calvin College in Grand Rapids, Michigan and is a registered Professional Engineer. As an inventor, Mr. DeVries has 17 patents and is an active member in Conveyor Equipment Manufacturers Association (CEMA), Society for Mining, Metallurgy & Exploration (SME), and ASME.

Brett DeVries  
Chief Engineer, R&D Department  
Flexible Steel Lacing Company (Flexco)  
Grand Rapids  
1995 Oak Industrial Dr. NE  
Grand Rapids, Michigan 49505  
USA  
Email: [BDevries@flexco.com](mailto:BDevries@flexco.com)